Influence of thickness of the porous layer on thin film condensation in forced convection in a canal whose walls are covered with a porous material: Determination of lengths of entry

Abstract – *We have numerically studied condensation by forced convection of the thin film type in a channel whose walls are covered with porous media.*
The generalized Darcy-Brinkman-Forchheimer (DBF) equations in the porous medium and those of the hydrodynamic and thermal boundary layers in the pure liquid were used and solved by the decentred implicit finite difference method and the iterative Gauss-Seidel method. After validating, the influence of the thickness of the porous layer on the longitudinal velocity *and the temperature profiles in the porous medium and in the pure liquid, the thickness of the liquid film, the local Nusselt number (the rate of heat transfer) and the lengths of entry have been studied.*
We note that an increase in the thickness of the porous layer increases the friction and decreases the contact of the fluid with the cold plate and allows a decrease in the longitudinal velocity *and an increase in the temperatures in the porous medium and the pure liquid, a decrease liquid film thickness (disadvantaged condensation) and increases the local Nusselt number (heat transfer rate at the porous medium/liquid film interface) and also an increase in the length of entry. The increase in length of entry is quasi-linear. The sensitivity of condensation to a change in thickness of the porous layer is constant.*

Keywords*: Channel with Porous Wall, Condensation Thin Film, Generalized Darcy-Brinkman- Forchheimer Model, iterative Gauss-Seidel relaxation method, Lengths of Entry, Thickness of the porous layer*

1. Introduction

Heat and mass transfer during the condensation of saturated steam in porous media are generally encountered in practise such in many technological fields: the thermics exchangers, the cooling of the electronic components, storage of energy, desalination, distillation, drying.

During the recent years the vapor condensation in a porous medium has received considerable attention in many theoretical and experimental investigations [1-19].

Shekarriz and Plumb [1] by examining the effect of the presence of porous medium on the condensation of the film on the external wall of a horizontal tube, showed that they contributed to significantly reducing the thickness of the liquid film. So it (the presence of porous medium) improves the heat exchange with the wall. By carrying out an analytical and numerical study of film condensation on a wall covered with an inclined porous material,

Chaynane R. and al. [2] presented a comparison between Darcy-Brinkman-Forchheimer (DBF) and Darcy-Brinkman (DB) models. They also investigated the effects of effective viscosity, permeability and dimensionless thickness of the porous coating on flow and heat transfer enhancement.

Asbik M and al. [3] compared the Darcy-Brinkman (DB) model and the Darcy-Brinkman-Forchheimer (DBF) model with analytical and numerical studies of a vapor condensation problem in a porous thin film. They presented in their results: the velocity and temperature profiles in the porous layer, the thickness of the liquid film, the local Nusselt number and the influences of the Reynolds and Darcy numbers and the dimensionless thickness of the porous layer.

Ndiaye M. and al. [4-7] studied the influences of the Prandtl, Froude, Reynolds and Jacob numbers, the dimensionless thickness of the porous layer and the thermal conductivity ratio on the transfers in the porous medium and in the liquid phase in proposing a model for the numerical study of the condensation of pure saturated vapor of the thin film type in forced convection on a wall covered with porous material.

Patil A.A. and al. [8] submitted a solar water distillation system with a combination of surface condenser and vacuum pump. They showed that the daily distillate production increases by up to 43% by coupling the surface condenser and the vacuum pump due to the increased rate of evaporation and condensation.

R.S. Jha and al. [9] exposed the numerical simulations based on the analytical modeling of the heat and mass transfer processes involved in the condensation of moisture in the flue gases in a tubular counter-current heat exchanger. They investigated operating parameters such as fluid flow inlet temperatures and flow ratio with the aim of achieving maximum heat and moisture recovery. They concluded that the rates of condensation and heat transfer increase considerably by increasing the flow ratio and decreasing the temperature of the incoming cooling water.

A. Nasr and S. Al-Ghamdi [10] showed that the presence of the porous layer enhances the heat and mass transfer performance at the liquid-gas interface during the liquid film evaporation in the free convection by proposing a numerical study of coupled heat and mass transfers during the evaporation of a flowing liquid film.

Abdelaziz Nasr [11] showed numerically that the performance of heat and mass transfer at the liquid-gas interface during the condensation of the liquid film is improved by the presence of the porous layer by studying a numerical model of heat and mass transfer enhancement of liquid film condensation by covering a porous layer on one of the vertical channel plates

Charef A. and al. [12] have numerically studied the condensation of the liquid film from vapor-gas mixtures of HFC refrigerants inside a vertical tube. They concluded that condensation of R152a-air corresponds to higher accumulated condensation mcd and local heat transfer coefficient hT compared to R134a-air under the same conditions.

Mosaad M. E-S. and al. [13] presented a model of a regular process of condensation of a laminar film on a vertical wall with the back face cooled by free convection in a porous medium saturated with fluid. The conjugate solution of the laminar film condensation problem is different from a Nusselt-type solution was concluded.

Charef A. and al. [14] presented a model on liquid film condensation in a thermal desalination process, which is based on the phase change phenomenon. First, they learned that increasing the temperature difference between the inlet and the wall improves the thickness of the condensate film. Decreasing the radius of the tube increased the process of condensation. The radius of the tube and the incondensable gas were finally retained as relevant factors to improve the efficiency of thermal desalination units.

Sellami K. and al [15] found that the evaporative cooler is more efficient for high porosity and thick porous medium, with up to 23% improvement for high porosity by numerically addressing the combined heat and mass exchanges in the process of direct evaporative cooler, from a porous media of laminar airflow between two parallel-insulated walls.

Ndiaye P.T. and al. [16] presented a numerical study of thin layer type condensation in forced vapor convection on a channel whose walls are covered with porous material. They studied the influence of Reynolds and Prandtl numbers. The increase in the Reynolds number and the Prandtl number led to an increase in the longitudinal velocity and the temperature, improves the heat exchanges at the interface of the porous medium and the liquid film (local Nusselt number).v

In their article, Ndiaye P.T. et al. [17-18] presented the numerical study of thin film type condensation in forced convection of pure saturated steam in a channel whose walls are covered with a porous material. By noting that the thickness of the two liquid films vary according to variable (parameters of the physical problem) and can meet, Ndiaye P.T. et al. [17, 18] studied this phenomenon (the meeting between the two liquid films) thanks to the length of entry, which will make it possible to determine the sensitivity of the condensation to a variation of a variable (or parameter of the physical problem). They studied the influence of Jacob numbers and ratio of form on flow, transfer and condensation.

Ndiaye G. and al. [19] worked on a study of forced convection condensation of a laminar film of a pure and saturated vapor on a porous plate inclined to the vertical. The effects of different

influential parameters such as: inclination, effective viscosity, and dimensionless thermal conductivity λ^* on the flow and heat transfers are presented.

As Ndiaye P. T. and al. [17, 18], in our case we will study this time the influence of the thickness of the porous medium instead of the Jacob number and a ratio of form on the flow , transfer and condensation (unlike Ndiaye P. T. et al. [17, 18]).

The hydrodynamic and thermal boundary layer equations will be employed in the pure liquid and will be used together with the generalized Darcy-Brinkman-Forchheimer (DBF) equations in the porous medium. To carry out this project well, first, we will proceed to the mathematical formulation with the descriptions of the simplifying hypotheses, the equations of the problem and the boundary conditions. Then announce the numerical resolution method. Finally evaluate the influence of the thickness of the porous medium on the velocity and temperature profiles in porous medium and pure liquid, the thickness of the liquid film, the local Nusselt number (the rate of heat transfer) and the lengths of entry (which characterizes condensation).

2. Mathematical formulation:

2.1 Physical model and assumptions :

This work focuses on the modeling of flows and transfers in porous media and pure liquids. To describe the resulting thin-film type condensation phenomenon, we consider the physical model (channel) and the coordinate system shown in Figure 1. This model is a channel formed by two flat, vertical, parallel plates, whose internal walls are covered with a porous material of permeability K and porosity ε, of thickness H. These plates are spaced apart by a distance 2A, of length L and are maintained at a temperature Tw lower than that of a saturated vapor TS which circulates at a uniform speed U0 at the entrance to the channel.

This results in a condensation of pure vapor on the porous medium and the presence of three zones:

(1) The porous medium saturated with the liquid

(2) The condensate film

(3) Pure saturated vapor.

The condensate film flows under the effect of the forces of gravity and viscous friction. (x, y) and (u, v) are respectively the Cartesian coordinates and the velocity components in the porous medium and the liquid in the coordinate system associated with the model.

This work focuses on the modeling of flows and transfers in porous media and pure liquids. To describe the thin-film type condensation that takes place, the channel (physical model) and the coordinate system schematized in Fig. 1 have been considered.

This channel is formed by two flat plates, vertical and parallel, the internal walls of which are covered with a porous material of permeability K and porosity ε, of thickness H. These plates are spaced apart by a distance 2A, of length L and are maintained at a temperature T_w lower than that of a saturated vapor T_S which flows at a uniform speed U_0 at the channel inlet.

There is a condensation of pure vapor on the porous medium and the existence of three zones:

(1) The porous medium saturated with the liquid

(2) The condensate film (pure condensed liquid)

(3) Saturated steam.

The condensate film flows under the effect of the forces of gravity and viscous friction. (x, y) and (u, v) are respectively the Cartesian coordinates and the velocity components in the porous medium and the liquid in the frame associated with the model.

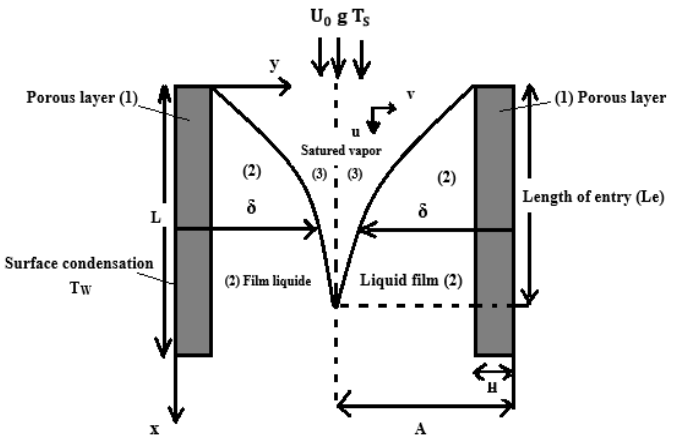

Fig 1 Geometry of the physical model and coordinate system

In order to achieve a coherent mathematical modeling of the physical problem and to reason the difficulties related to the resolution of the governing equations of the phenomenon, we considered the following simplifying hypotheses:

1-The hydrodynamic and thermal boundary layer approximations are valid.

2--The matrix or porous material is isotropic and homogeneous.

3-The porous medium is saturated with a fluid (pure saturated vapor) supposed Newtonian and incompressible (where the equations of the flow and transfer in the vapor phase (3) are generally neglected).

4-The generated flow is permanent, laminar and two-dimensional

5-The working, induced by the viscous and pressure forces, is negligible.

6-The thermo-physical properties of the fluids and the ones of the porous matrix are assumed to be constant in the studied temperature range (the imposed temperature variations do not modify the thermo-physical properties of the fluid which remain constant).
7-The generalized model of Darcy-Brinkman-Forchheimer (DBF) is used to describe the flow in the porous layer.
8. Condensation occurs in the form of a thin film of greater thickness than the porous material
9-The porous matrix is in local equilibrium with the condensate.
10-The liquid-vapor interface is in thermodynamic equilibrium.
11- The solid and the fluid phases of the porous medium are in thermal equilibrium
12-The transverse and the longitudinal variation of the pressure is not taken into account in the porous matrix.
13-The transfer of energy by radiation is neglected
14-The geometry of the problem makes the flow considered axisymmetric.

2.2 Dimensionless Equations, Determination of local Nusselt number and length of entry

In the domains (1) and (2) already defined, the equations which govern the transfers and the boundary conditions associated with them have been made dimensionless by using the following variables and parameters, we pose:

$$x^* = \frac{x}{L} \quad (1) \quad ; \quad y^* = \frac{y}{A} \quad (2) \quad ; \quad H^* = \frac{H}{A} \quad (3) \quad ; \quad \delta^* = \frac{\delta}{A} \quad (4) \; ; \quad u^* = \frac{u}{U_0} \quad (5)$$

$$v^* = \frac{v}{U_0} \quad (6) \quad ; \quad \theta = \frac{T - T_w}{T_s - T_w} \quad (7) \quad ; \quad \lambda^* = \frac{\lambda_l}{\lambda_{eff}} \quad (8) \quad ; \quad \nu^* = \frac{\nu_{eff}}{\nu_l} \quad (9)$$

The dimensionless physical domain (x*,y*) thus obtained presents a curvilinear interface (liquid/pure vapor interface), we will transform it into a rectangular domain ($\boldsymbol{X}$,$\boldsymbol{\eta}$) in which the boundary and the interfaces (porous medium interfaces /pure liquid and pure liquid/vapour) will be identified by lines of constant coordinates. The following change (homotopic transformation) of variable is made:

$$\begin{cases} X = x^* \\ \eta = coef.\dfrac{y^*}{H^*} + (1 - coef)\left\{1 + \dfrac{y^* - H^*}{\delta^*(X) - H^*}\right\} \end{cases} \qquad (10)$$

With *Coef* it is a coefficient equal to 1 in the porous layer and 0 in the pure liquid. Thus the frame (x*, y*) is transformed into a rectangular field ($\boldsymbol{X}$, $\boldsymbol{\eta}$). The porous medium / pure liquid interface is parametrized by the straight line with coordinate η = 1 and the pure liquid / vapor interface is parametrized by the straight line with coordinate η = 2.

In both media, the dimensionless equations in the rectangular domain ($\boldsymbol{X}$, $\boldsymbol{\eta}$) are written:

Porous layer: $0 \le \eta \le 1$

The equation of conservation of mass or equation of continuity is:

$$\frac{\partial u^*_p}{\partial X} + \frac{L}{A}\frac{1}{H^*}\frac{\partial v^*_p}{\partial \eta} = 0 \quad (11)$$

The equation of momentum following X-direction is:

$$u^*_p \frac{\partial u^*_p}{\partial X} + \frac{L}{A}\frac{v^*_p}{H^*}\frac{\partial u^*_p}{\partial \eta} = \frac{\varepsilon^2}{Fr} - \varepsilon^2\left(\frac{L}{A}\right)^2 \frac{\nu^*.Da}{\mathrm{Re}} u^*_p + \varepsilon^2\left(\frac{L}{A}\right)^2 \nu^* \frac{1}{\mathrm{Re}H^{*2}}\frac{\partial^2 u^*_p}{\partial \eta^2} - \varepsilon^2 F\sqrt{Da}\frac{L}{A}u^{*2}_p \quad (12)$$

The equation of heat is:

$$u^*_p \frac{\partial \theta_p}{\partial X} + \frac{L}{A}\frac{v^*_p}{H^*}\frac{\partial \theta_P}{\partial \eta} = \left(\frac{L}{A}\right)^2 \frac{1}{\mathrm{RePr}_{eff} H^{*2}}\frac{\partial^2 \theta_P}{\partial \eta^2} \quad (13)$$

Pure liquid: $1 \prec \eta \prec 2$

The equation of conservation of mass or equation of continuity is:

$$\frac{\partial u^*_l}{\partial X} - \frac{(\eta - 1)}{\left(\delta^*(X) - H^*\right)}\frac{d\delta^*(X)}{dX}\frac{\partial u^*_l}{\partial \eta} + \frac{L}{A}\frac{1}{\left(\delta^*(X) - H^*\right)}\frac{\partial v^*_l}{\partial \eta} = 0 \quad (14)$$

The equation of momentum following X-direction is:

$$u^*_l\left[\frac{\partial u^*_l}{\partial X} - \frac{\eta - 1}{\delta^*(X) - H^*}\frac{d\delta^*(X)}{dX}\frac{\partial u^*_l}{\partial \eta}\right] + \frac{L}{A}\frac{v^*_l}{\delta^*(X) - H^*}\frac{\partial u^*_l}{\partial \eta} = \left(\frac{L}{A}\right)^2 \frac{1}{\mathrm{Re}\left(\delta^*(X) - H^*\right)^2}\frac{\partial^2 u^*_l}{\partial \eta^2} + \frac{1}{Fr}\left(1 - \frac{\rho_v}{\rho_l}\right) \quad (15)$$

The equation of heat is:

$$u^*_l\left[\frac{\partial \theta_l}{\partial X} - \frac{\eta - 1}{\delta^*(X) - H^*}\frac{d\delta^*(X)^*}{dX}\frac{\partial \theta_l}{\partial \eta}\right] + \frac{L}{A}\frac{v^*_l}{\delta^*(X) - H^*}\frac{\partial \theta_l}{\partial \eta} = \left(\frac{L}{A}\right)^2 \frac{1}{\mathrm{Re}\,\mathrm{Pr}\left(\delta^*(X) - H^*\right)^2}\frac{\partial^2 \theta_l}{\partial \eta^2} \quad (16)$$

To these equations are added the following boundary and dimensionless continuity conditions:

Conditions at the entry: $X = 0$

$$u^*_p(0,\eta) = 1 \quad (17) \quad ; \quad v^*_p(0,\eta) = 0 \quad (18) \quad ; \quad \theta_p(0,\eta) = 1 \quad (19)$$

Boundary conditions at the wall**:** $\eta = 0$

$$u^*_p = v^*_p = 0 \quad (20); \quad \theta_p = 0 \quad (21); \quad u^*_p = v^*_p = 0 \quad (22); \quad \theta_p = 0 \quad (23)$$

At the porous/pure liquid interface: $\eta = 1$

$$u_l^* = u_p^* \quad (24) \quad ; \quad \theta_l = \theta_p \quad (25)$$

Continuity of constraints

$$\frac{\mu^*}{H^*}\frac{\partial u_p^*}{\partial \eta} = \frac{1}{\left(\delta^*(X) - H^*\right)}\frac{\partial u_l^*}{\partial \eta} \quad (26)$$

Continuity of thermal flows:

$$\frac{1}{H^*}\frac{\partial \theta_p}{\partial \eta} = \frac{\lambda^*}{\left(\delta^*(X) - H^*\right)}\frac{\partial \theta_l}{\partial \eta} \quad (27)$$

At the liquid / vapor interface $\eta = 2$

$$\theta_l = 1 \quad (28) \; ; \quad \frac{\partial u_l^*}{\partial \eta} = 0 \quad (29)$$

The dimensionless speed and temperature depending on the thickness of the liquid film, the heat and mass balances can be coupled. The coupled equation of mass flow and heat balance made dimensionless is expressed by the following relationship:

$$\left(\frac{L}{A}\right)^2 \frac{Ja}{(Pe)_{eff}}\frac{1}{H^*}\frac{\partial \theta_p}{\partial \eta}\Big/_{\eta=0} = \frac{d}{dX}\left\{(1+Ja)\delta^*(X)\frac{\rho_v}{\rho_l}\right\} - Ja\frac{d}{dX}\left\{H^*\int_0^1 \theta_p u_p^* d\eta + \left(\delta^*(X) - H^*\right)\int_1^2 \theta_l u_l^* d\eta\right\} \quad (30)$$

With:

The mass flow rate:

$$H^*\int_0^1 u_p^* d\eta + \left(\delta^*(X) - H^*\right)\int_1^2 u_l^* d\eta = \frac{\rho_v}{\rho_l}\delta^*(X) \quad (31)$$

Number of Jacob:

$$Ja = \frac{Cp_l (T_S - T_W)}{h_{fg}} \quad (32)$$

Number of Froude:

$$Fr = \frac{U_0^2}{gL} \quad (33)$$

Number of Reynolds:

$$\mathrm{Re} = \frac{U_0 L}{\nu_l} = \nu^* . \frac{U_0 L}{\nu_{eff}} \quad (34)$$

Number of Darcy:

$$Da = \frac{A^2}{K} \quad (35)$$

Number of Prandtl:

$$\Pr = \frac{\nu_l}{\alpha_l} = \frac{\mu_l C_{p_l}}{\lambda_l} \qquad (36)$$

Number of Peclet:

$$Pe = \mathrm{Re}.\Pr \qquad (37)$$

Number of Peclet modified:

$$Pe_{eff} = \lambda^* Pe = \lambda^* \mathrm{Re}.\Pr \qquad (38)$$

Number of de Prandtl modified:

$$\Pr_{eff} = \lambda^* \Pr \qquad (39)$$

Determination of the Lengths of Entry (Le)

The length of entry already defined by Ndiaye P. T. and al. [16]: 'The length of entry (Le) is defined as the length from the channel inlet to the meeting of the two liquid films. This is the length of the channel from which the boundaries layers conditions are not applicable anymore [16].

$$\delta(x = Le) = A \qquad (41)$$

In dimensionless form and a rectangular domain, it is:

$$\delta^*(X = Le^*) = 1 \qquad (42)$$

The partial differential equations which govern our problem are not only nonlinear, coupled between them, also coupled with their boundary conditions. They generally do not have analytical solutions, except for very simplified cases. The use of numerical methods becomes inevitable for complex cases closer to reality.

3. NUMERICAL METHODOLOGY

Numerical resolutions include two steps: a meshing step and a discretization step. The transfer equations are discretized by an implicit finite difference method.

The transfer equations are discretized by an implicit finite difference method. The advection terms are discretized respectively with a backward off-center scheme and the diffusion terms are discretized respectively with a centered in order to make possible the main diagonals of the most dominant matrices possible (for more stability).

We used a double-scan method combined with an iterative Gauss-Seidel type line-by-line sub-relaxation scheme to solve numerically the systems of coupled algebraic equations thus obtained. We have defined the relaxation coefficients empirically to guarantee the non-growth of calculation errors during the iterative process, which will make our diagrams stable and

convergent. For the local Nusselt number (heat transfer rate), a second order progressive finite difference scheme will be used for more precision.

4. RESULTS AND DISCUSION

4.1 Results of method validation:

We validated our model by comparing it to the work of Ndiaye et al. [4-7].
For this we considered the same conditions as him, a low number (*Re = 2*). Because Ndiaye M. (2014) had retained that his model was only valid for values of the Reynolds number lower than 7. As we considered two characteristic lengths L and A to make our model dimensionless, we will consider them equal *(L/A = 1)* because they [4-6] had a single characteristic length and low permeability, therefore a high Darcy number ($Da = 10^{12}$).
For the study of the sensitivity of the mesh we chose $\Delta X = 0.0001$ and $\Delta\eta = 0.02$ to respond at the same time to the speed, the precision and the convergence of the calculations to answer at the same time the speed, the precision and convergence of calculations.

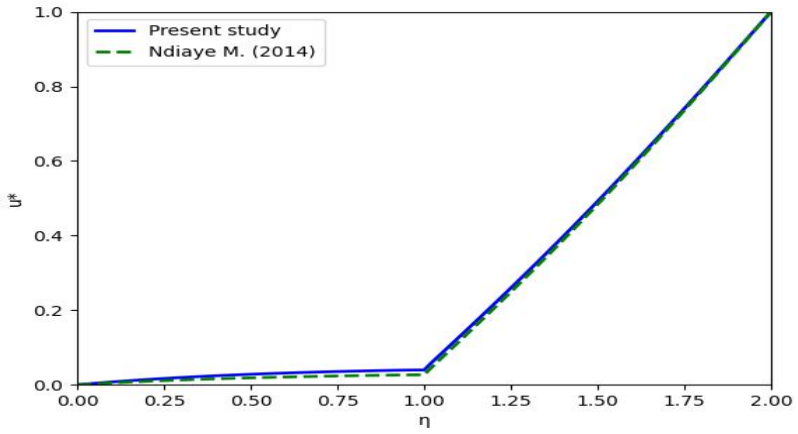

Fig. 2: Comparison of the velocity profile of our study with that of Ndiaye M. and al. [4-6]

Re=2; Fr=10^{-4} ; λ^*=2.9; H^*=2.10^{-3}; Ja=10^{-3} ; v^*=1; L/A=1; Da=10^{12}; Ɛ=0.4; F=0.55

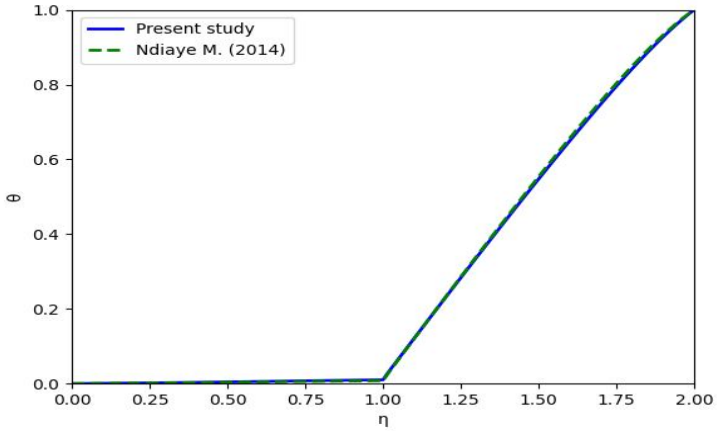

Fig. 3: Comparison of the temperature profile of our study with that of Ndiaye M. and al. [4-6]

Re=2; Fr=10^{-4} ; λ^*=2.9; H^*=2.10^{-3}; Ja=10^{-3} ; v^*=1; L/A=1; Da=10^{12}; ; Ɛ=0.4; F=0.55

We note a small superiority of the dimensionless longitudinal velocity, particularly in the porous medium of our study (compared to the model of Ndiaye M. et al. [4-6], which is due to the inertial effects that we took into account in the porous medium (unlike Ndiaye M. et al. [4-6]) which are not predominant in our case (because Re = 2, Re is low) (Fig. 2) We can retain a good agreement for the dynamic field (Fig. 2). a very good agreement is noted for the thermal field despite the slight superiority of the values of our dynamic field (Fig. 3). Because advection is negligible with low values of the Reynolds number. The agreement is good, our model is valid.

4.2- Results and discussions

In this study the influence of the thickness of the porous layer on the behavior longitudinal velocity, the temperature, the thickness of film, the thermal rate of transfer (local Nusselt number) and finally over the length of entry will be shown.

The results from the numerical simulations are related to : Ɛ=0.4; F=0.55; υ^*=1; Da=10^9; λ^* =3; Fr=10^{-4}

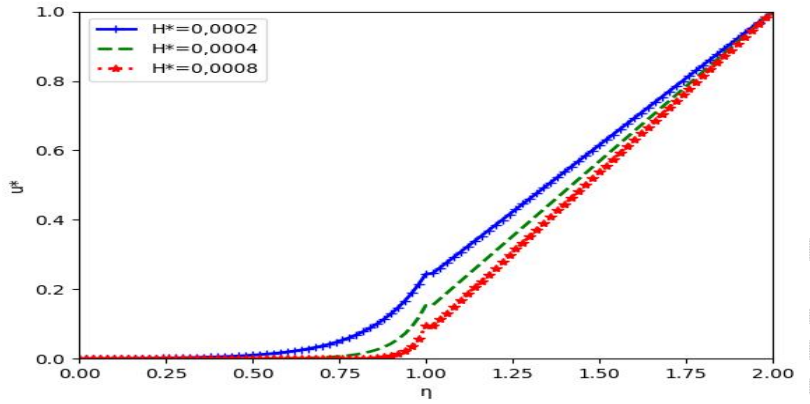

Fig. 4: Variation of the longitudinal velocity as a function of the ordinate η for different values of H* at the position X= 0.05.

Re=200; Pr=5; L/A =25 ; Ja=10^{-8}

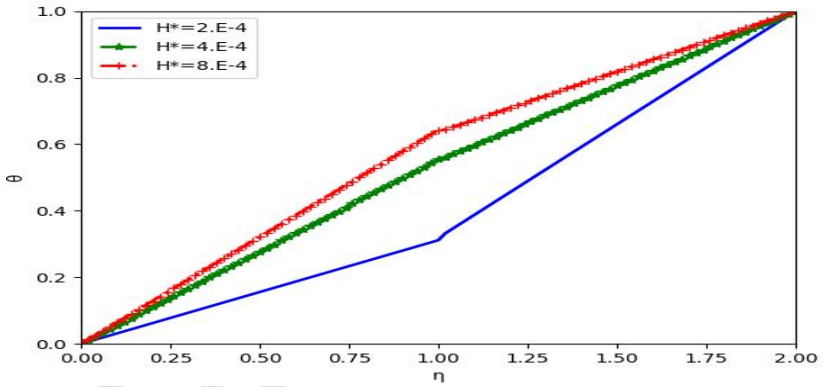

Fig. 5: Variation of the longitudinal temperature as a function of the ordinate η for different values of H* at the position X= 0.05.

Re=200; Pr=5; Ja=10^{-7} ; L/A =75 ; Ja=10^{-7}

The longitudinal velocity decreases as the thickness of the porous layer increases (Fig. 4). The presence and increase in the thickness of the porous layer perturbs the flow by its friction. We notice an increase in temperature with increasing dimensionless thickness of the porous layer (Fig. 5). Indeed, the increase in the porous coating decreases the contact between the fluid and the (cold) condensation plates, which increases the temperature.

Fig. 6 shows an increase in the thickness of the condensate film as the thickness of the porous layer decreases. It can be interpreted by the fact that the decrease in the thickness of the porous layer allows better contact with the cold plate. This promotes condensation and therefore increases the thickness of the liquid film.

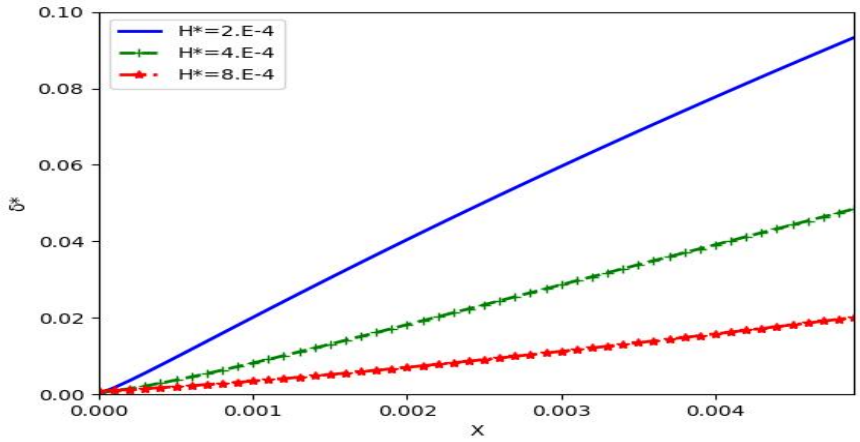

Fig. 6: Variation of the thickness of the liquid film as a function of the abscissa X for different values H*

Re=25; Pr=5; L/A =150 ; Ja=10^{-7}

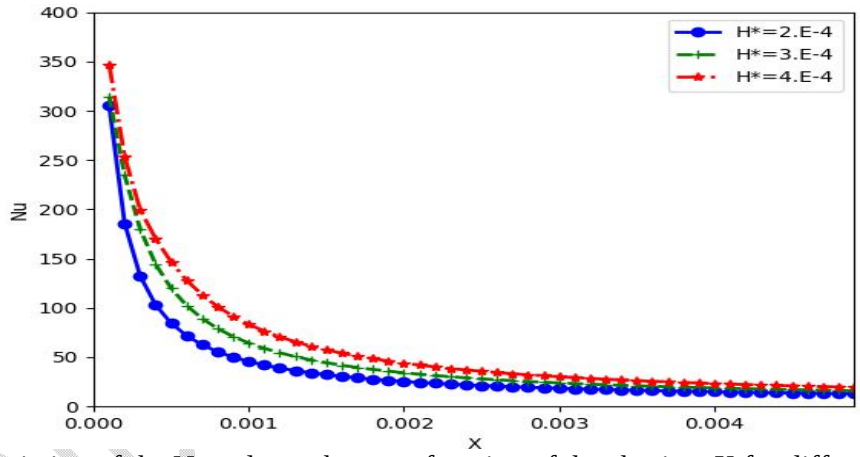

Fig. 7: Variation of the Nusselt number as a function of the abscissa X for different values of H*

Re=25; Pr=2 ; L/A =200 ; Ja=10^{-7}

The local Nusselt number, rate of heat transfer at the porous medium/pure liquid interface, is the ratio of the total heat transfer to the transfer by conduction. When the local Nusselt number is low, much of the heat transfer is by conduction with no flux or very low flux because there is little convection. When the Nusselt number is large, transfer by convection is active. We study the variation of the Nusselt number as a function of the abscissa X. We note the value of the Nusselt number is very large at the entrance of the channel, then decreases rapidly along the porous wall to reach very low asymptotic values. The heat transfer by conduction (weak at the entrance of the channel) gradually increases along the porous wall on

the convective heat transfer, which explains a decrease in the Nusselt number as a function of the abscissa X. that the fluid descends along the abscissa X in the channel; its temperature tends towards that of the plates and the temperature gradients become weaker. The local Nusselt number decreases along X (along the channel). An increase in the Nusselt number is noted with the increase in the thickness of the porous layer (Fig. 7).

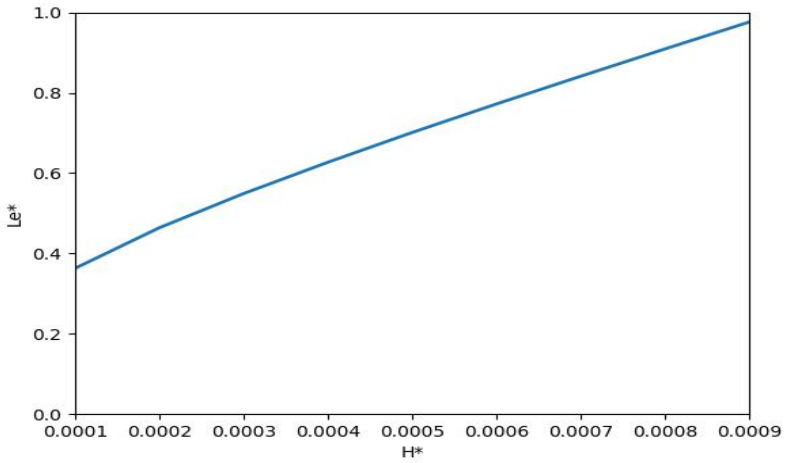

Fig. 8: variation of the dimensionless length of entry ($\boldsymbol{Le}^*$) as a function of H*

Re=50; Pr=3; Ja=10^{-7}; L/A=100

The variation of the dimensionless lengths of entry highlights the ease of variation of the dimensionless liquid film thickness which depends exclusively on condensation. Thus, the variations of the lengths of entry as a function of the thickness of the porous layer (Fig. 8) make it possible to characterize the sensitivity of the condensation to a variation of the thickness of the porous layer. An increase in the thickness of the liquid film (promoted condensation) leads to a decrease in the lengths of entry and respectively its decrease increases the lengths of entry. Hence the variations of the dimensionless lengths of entry (Fig. 8) confirm those of the dimensionless thickness of the liquid film (Fig. 6).

Figure 8 shows an increase in length of entry as a function of dimensionless porous layer thickness. This increase is almost linear unlike Ndiaye P. T. and al. [17-18] (Variations in the dimensionless length of entry according to the Jacob number and ratio of form). Here, the sensitivity of the condensation to a change in thickness of the dimensionless porous layer is constant whatever its value (thickness of the porous layer).

5. Conclusion

We have studied forced convection condensation of the thin film type. Our equations (generalized Darcy-Brinkman-Forchheimer (DBF) equations in the porous medium and those

of the hydrodynamic and thermal boundary layers in pure liquid) were solved using the decentered implicit finite difference method. The advection terms are discretized with a backward-centered scheme and the diffusion terms with a centered scheme.

After validating our model in comparison to Ndiaye M. [4-7], the influence of the thickness of the porous layer on the longitudinal velocity, the temperature profiles in the porous medium and in the pure liquid, the thickness of the liquid film , the local Nusselt number (the rate of heat transfer) and the lengths of entry have been studied.

It is found that an increase in the thickness of the porous layer increases the friction and decreases the contact of the fluid with the cold plate and allows a decrease in the speed and an increase in the temperatures in the porous medium and the pure liquid, a decrease liquid film thickness (disadvantaged condensation) and increases the local Nusselt number (heat transfer rate at the porous medium/liquid film interface) and also an increase in the dimensionless length of entry. The increase in length of entry is quasi-linear. The sensitivity of condensation to a change in thickness of the dimensionless porous layer is constant.

Nomenclature

Greeks symbols
α: thermal diffusivity, m2.s-1
δ thickness of condensate, m
ε : Porosity
η : dimensionless coordinate in the transverse direction
θ : temperature dimensionless
λ : thermal conductivity, W.m-1.K-1
μ : viscosité dynamique, kg.m-1.s-1
ν : dynamic viscosity, m2.s-1
ρ : density, kg.m-3
Latines letters:
A: half-width of the channel, m
Cp: specific heat, J.kg-1. K-1
Da: Darcy's number
F: Forchheimer coefficient
Fr: Froude number
g: gravitational acceleration, m.s-2
H: thickness of the porous layer, m
hfg: enthalpy of evaporation, J.kg-1
Ja: Jacob number
K: hydraulic conductivity or permeability, m2
L: length of the plates of the channel, m
Nu: local Nusselt number
Pe: Peclet number
Pr: Prandtl number
Re: Reynolds number
T: temperature, K
u: velocity along x, m.s-1
U0: velocity of the free fluid (at the entrance of the channel), m.s-1
v: velocity along y, m.s-1
x, y: Cartesian coordinates, m
X: dimensionless coordinate in the longitudinal direction
Subscripts:
eff: effective value
int: porous substrate / pure liquid interface
l: liquid
p: porous
s: saturation
v: steam (vapor)
w: wall
*: dimensionless quantity

References

[1] Shekarriz A. and Plumb O.-A, Enhancement of film condensation using porous fins, *J. Thermo physics and heat Transfer, Vol. 3*, 1989, pp. 309-314.

[2] Chaynane R., Asbik M., Boushaba H., Zeghmati B., Khmou A. , Study of the laminar film condensation of pure and saturated vapor on the porous wall of an inclined plate. *Mechanics & Industries, Vol. 5*, No. 4, 2004, pp. 381-391

[3] Asbik M., Chaynane R., Boushaba H., Zeghmati B. and Khmou A., Analytical investigation of forced convection film condensation on a vertical porous-layer coated surface, *Heat and Mass Transfer, Vol. 40* (1-2*)* , 2003, pp. 143 – 155.
DOI 10.1007/s00231-002-0406-8

[4] Momath Ndiaye, Cheikh Mbow, Joseph Sarr, Belkacem Zeghmati, Modou Faye, Numerical Investigation of Laminar Forced Thin Film Condensation of a Saturated Vapor along a Vertical Wall Covered with a Porous Material: Effect of Prandtl and Froude numbers, *International Journal on Heat and Mass Transfer Theory and Applications (IREHEAT) , Vol. 1* N. 6, December 2013, pp 339-344.

[5] Momath Ndiaye, Cheikh Mbow, Joseph Sarr, Belkacem Zeghmati, Numerical Study of the Thin Film-type Condensation of Saturated Forced into a Vertical Wall Covered with a Porous Material Vapor Convection. *International Journal on Heat and Mass Transfer Theory and Applications (*IREHEAT), Vol. 1 N. 6, December 2013, pp 330-338.

[6] Momath NDIAYE, Cheikh MBOW, Joseph SARR, Numerical Investigation of Laminar Forced Thin Film Condensation of a Saturated Vapor along a Vertical Wall Covered with a Porous Material, *3rd International Francophone Symposium on Energy and Mechanics, Renewable Energies and Mechanics Applied to Industry*, pp. 211-216 des Actes, 5-6-7 May 2014, Moroni (Comores) CIFEM 2014.

[7] Momath NDIAYE**,** *Numerical Study of the Thin Film-type Condensation of Saturated Forced into a Vertical Wall Covered with a Porous Material Vapor Convection*, Ph.D. dissertation, Dpt of Physics, Cheikh Anta Diop University, Dakar, Senegal, 2014.

[8] Atul A. Patil, Atul, Tejas G. Patil, Aniruddha Y. Chaudhari, Performance Evaluation of Passive Solar Water Distillation System with Separate Surface Condenser and Vacuum Pump, *International Review of Mechanical Engineering (IREME), Vol. 11*, No 7, 467-(472) july 2017
10.15866/ireme.v11i7.12877

[9] Jha, R., Haribhakta, V., Kolte, A., Shekhadar, S., Tengale, S., Tare, S., Design and Simulation of Condensing Heat Exchanger, (2017) *International Review of*

Mechanical Engineering (IREME), vol. 11, No. 7, 2017, pp. 473-480. http://dx.doi.org/10.15866/ireme.v11i7.12879

[10] A. Nasr, S. Al-Ghamdi, A, Numerical study of evaporation of falling liquid film on one of two vertical plates covered with a thin porous layer by free convection, *Int J Therm Sci* 112 (2017) pp.335–344.

[11] Abdelaziz Nasr, Heat and mass transfer for liquid film condensation along a vertical channel covered with a thin porous layer, *International Journal of Thermal Sciences*, 124 (2018) 288-299.
http://dx.doi.org/10.1016/j.ijthermalsci.2017.10.016

[12] Charef A, Feddaoui M, Najim M, Meftah H. Comparative study during condensation of R152a and R134a with presence of non-condensable gas inside a vertical tube. *Heat and Mass Transfer*. 2018;54:1085-1099.
https://doi.org/10.1007/s00231-017-2205-2

[13] Mohamed El-Sayed MOSAAD and Rashed AL-AJMI, film condensation generated by free convection in a porous medium, *THERMAL SCIENCE*, *Vol. 22*, No. 6B, Year 2018, pp. 2699-2710. https://doi.org/10.2298/TSCI160820316M

[14] Adil Charef, M'barek Feddaoui, Abderrahman Nait Alla, Monssif Najim, Computational Study of Liquid Film Condensation with the Presence of Non-Condensable Gas in a Vertical Tube, *Desalination and Water Treatment*, Chapter 4, November 5th 2018, pp.55-76.
http://dx.doi.org/10.5772/intechopen.76753

[15] Karima Sellami, Nabila Labsi, Monssif Najim, Youb Khaled Benkahla, Numerical Simulations of Heat and Mass Transfer Process of a Direct Evaporative Cooler From a Porous Layer, *Journal of Heat Transfer, Vol. 141* / 071501, JULY 2019
[DOI: 10.1115/1.4043302]

[16] Ndiaye P. T., Ndiaye M., Mbow C., Ndiaye G.,, "Influence of Reynolds and Prandtl Numbers on Thin Film Condensation in Forced Convection in a Canal Covered with a Porous Material". International Journal on Engineering Applications (IREA), Vol 8, n. 5, pp 178-187, September 2020. https://doi.org/10.15866/irea.v8i5.18678

[17] Ndiaye P. T., Ndiaye M., Mbow C., Ndiaye G., "Numerical Study of Thin Film Condensation in Forced Convection in a Canal whose Walls Are Covered with a Porous Material: Influence of Jacob Number- Determination of Lengths of entry". International Journal on Engineering Applications (IREA), Vol. 8, n.4, pp 125-132, July 2020. https://doi.org/10.15866/irea.v8i4.18687

[18] Ndiaye P. T., Ndiaye M., Ndiaye G., Mbow C., "Numerical Study of Thin Film Condensation in Forced Convection in a Canal Whose Walls Are Covered with a Porous Material: Influence of ratio of form-Determination of Lengths of Entry". Journal of Chemical, Biological and Physical Sciences An International Peer Review E-3 Journal of Sciences Available online at www.jsbsc.org Section C: Physical Sciences, JCBPS; Section C; May 2022 –July 2022, Vol. 12, No. 3; 166-180.
DOI: 10.24214/jcbps.C.12.3.16680

[19] Ndiaye, G., Sambou,V., Ndiaye, M. and Ndiaye, P.T. (2022) Numerical Study of Thin Film Condensation in Forced Convection on an Inclined Wall Covered with a Porous Material. Open Journal of Applied Sciences, 12, 793-805. https://doi.org/10.4236/ojapps.2022.125053

,